Electronic Supporting Information for

Insights into Mechanism and Aging of a noble-metal free H_2-evolving Dye-Sensitized Photocathode

Nicolas Kaeffer,[1†] Christopher D. Windle,[1†] Romain Brisse,[2] Corinne Gablin,[3] Didier Leonard,[3] Bruno Jousselme,[2] Murielle Chavarot-Kerlidou[1] and Vincent Artero*[1]

[1]Laboratoire de Chimie et Biologie des Métaux, Université Grenoble Alpes, CNRS UMR 5249, CEA, 17 rue des Martyrs, F-38054 Grenoble, Cedex, France

[2]Laboratory of Innovation in Surface Chemistry and Nanosciences (LICSEN), NIMBE, CEA, CNRS, Université Paris-Saclay, CEA Saclay, 91191 Gif-sur-Yvette, Cedex, France.

[3]Univ Lyon, CNRS, Université Claude Bernard Lyon 1, ENS de Lyon, Institut des Sciences Analytiques, UMR 5280, 5, rue de la Doua, F-69100 Villeurbanne, France.

*to whom correspondence should be addressed. E-mail address: vincent.artero@cea.fr, www.solhycat.com

†These authors contributed equally

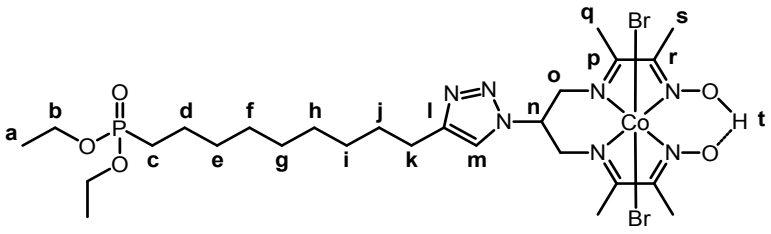

Co_{C11PEt}

Figure S1. Atoms numbering in $Co_{C_{11}PEt}$

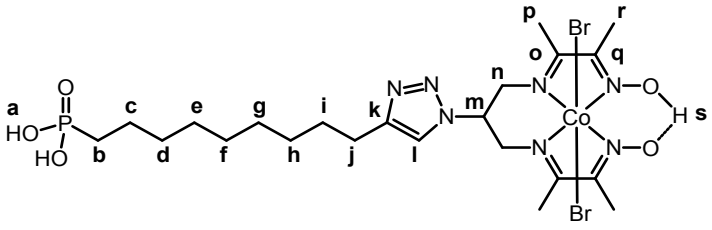

Co_{C11P}

Figure S2. Atoms numbering in $Co_{C_{11}P}$

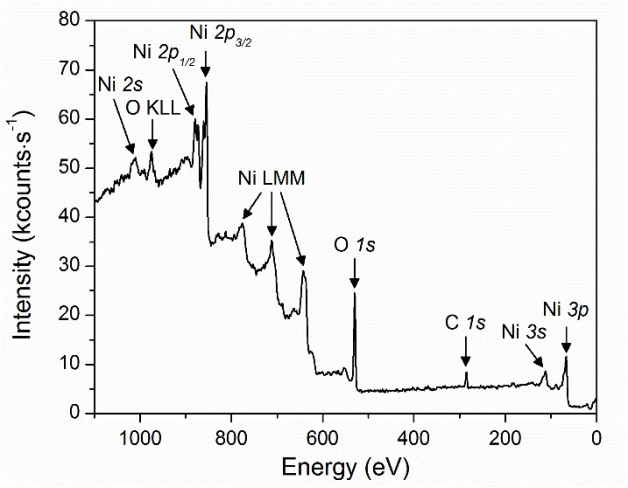

Figure S3. XPS analysis of a Dyenamo **NiO** electrode sintered at 450°C. The core levels of Ni and of O represent main features displayed on the spectrum. The C *1s* peak was used as a reference (at 284.8 eV) for the energy calibration. The presence of carbon is either adventitious (from an external contaminant) and/or residual from the preparation of NiO.

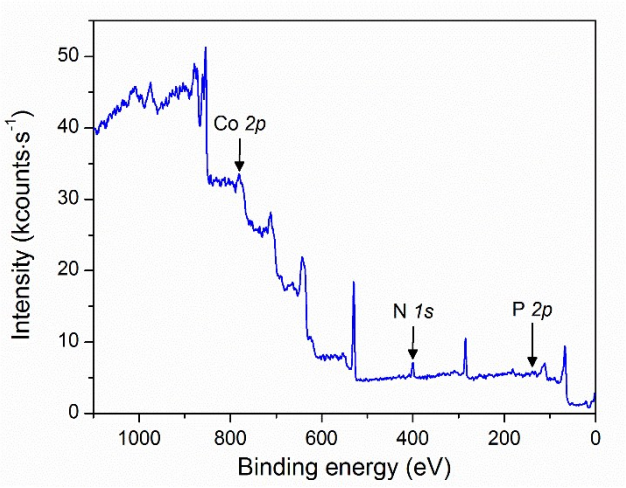

Figure S4. XPS analysis of a **NiO|Co$_{C_{11}P}$** electrode in the survey mode.

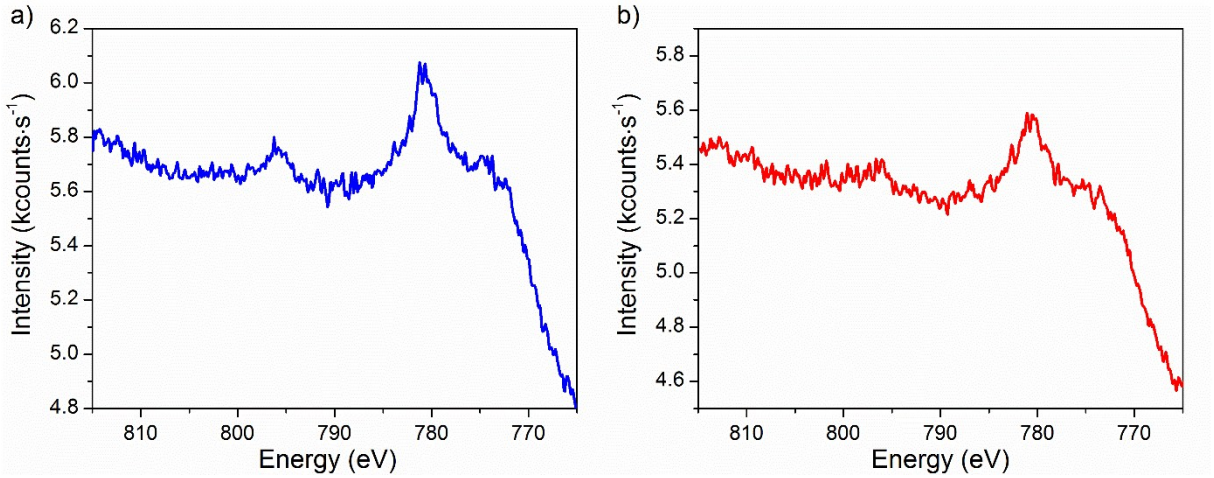

Figure S5. High resolution XPS analyses of the a) **NiO|Co$_{C_{11}P}$**, and b) **NiO|RBG-174|Co$_{C_{11}P}$** electrodes at the baseline-corrected Co *2p* core levels.

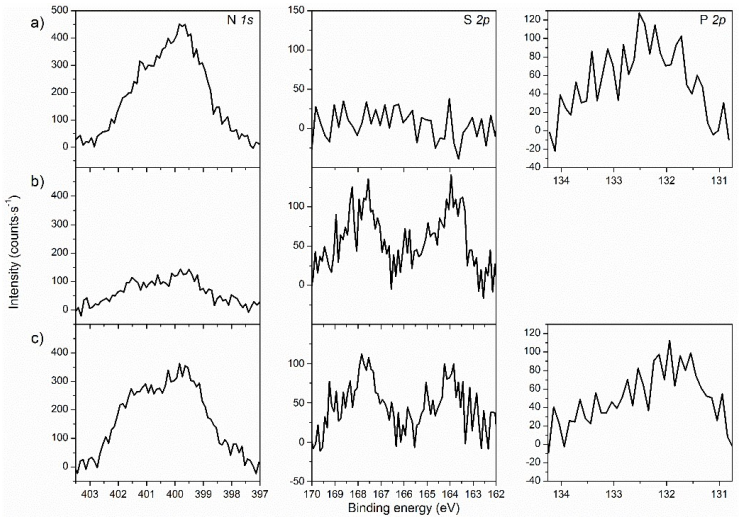

Figure S6. High resolution XPS analyses of the a) **NiO|Co$_{C_{11}P}$**, b) **NiO|RBG-174** and c) **NiO|RBG-174|Co$_{C_{11}P}$** electrodes at the baseline-corrected N *1s*, S *2p* and P *2p* core levels.

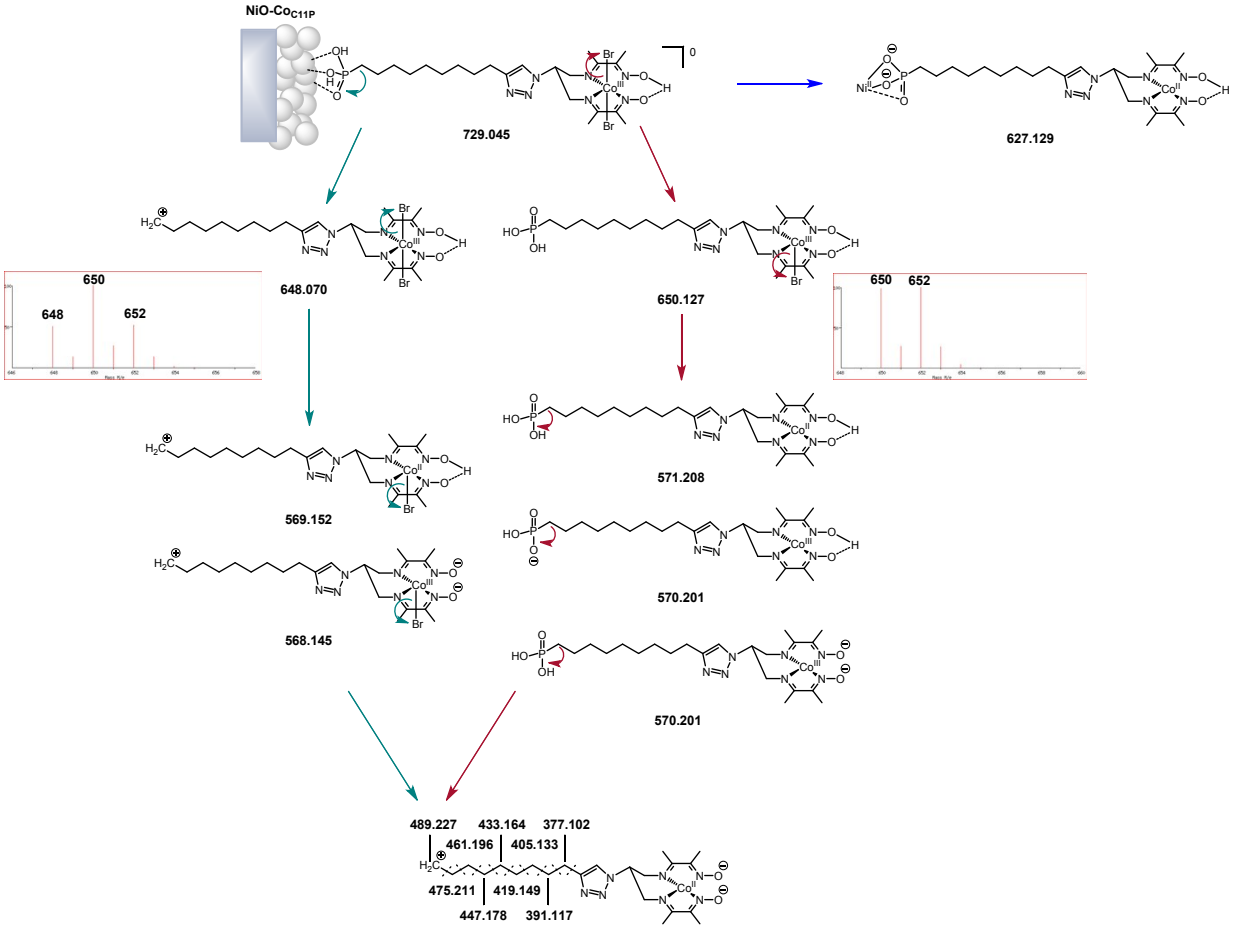

Figure S7. Proposed fragments (with corresponding exact masses) for the attribution of the main peaks detected in the ToF-SIMS positive mode spectrum at a **NiO|Co$_{C_{11}P}$** electrode. The secondary ions are monocharged cations; their charges are not shown for the sake of clarity.

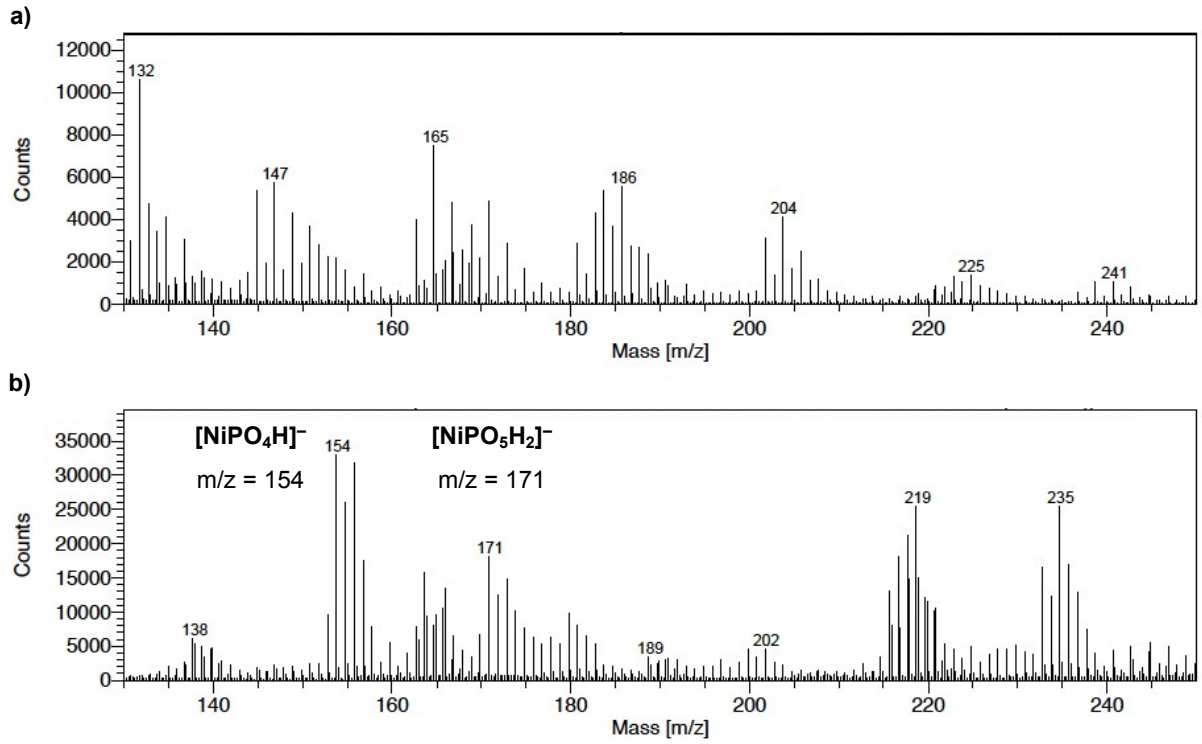

Figure S8. Negative mode ToF-SIMS spectra in the m/z 150-250 range for **a)** NiO blank and **b) NiO|RBG-174|$Co_{C_{11}P}$** electrodes.

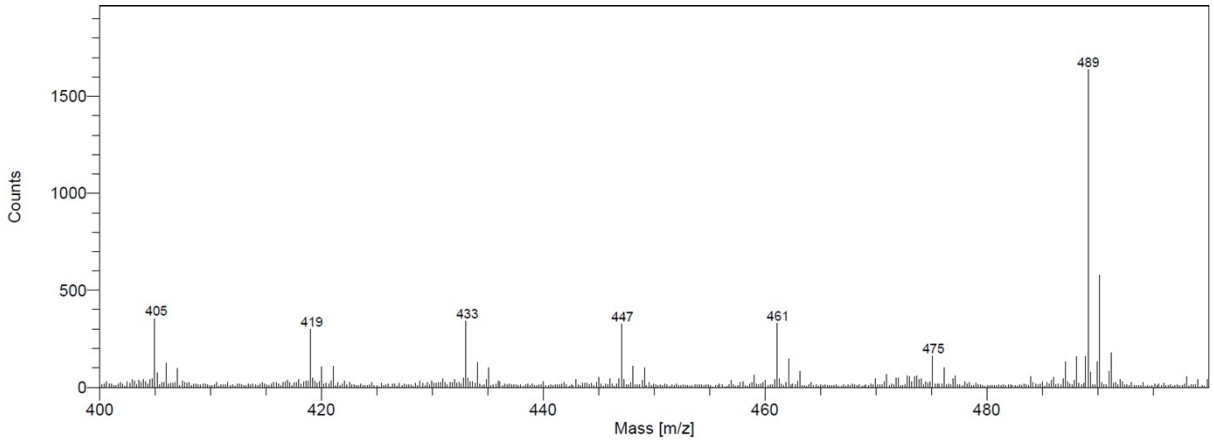

Figure S9. ToF-SIMS analysis at the surface of the **NiO|$Co_{C_{11}P}$** electrode recorded in the positive mode in the m/z range 400-500.

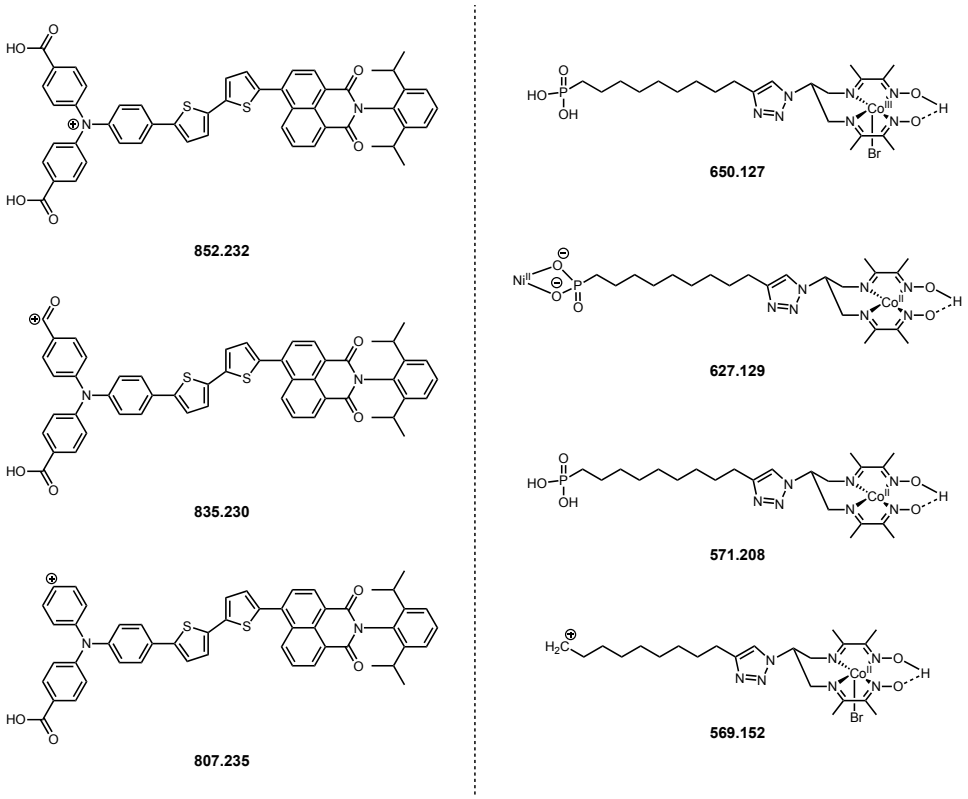

Figure S10. Proposed fragments (with corresponding exact masses) for the attribution of the main peaks detected in the ToF-SIMS positive spectrum of the **NiO|RBG-174|Co$_{C_{11}P}$** electrode. The secondary ions are monocharged cations; their charges are not shown for the sake of clarity.

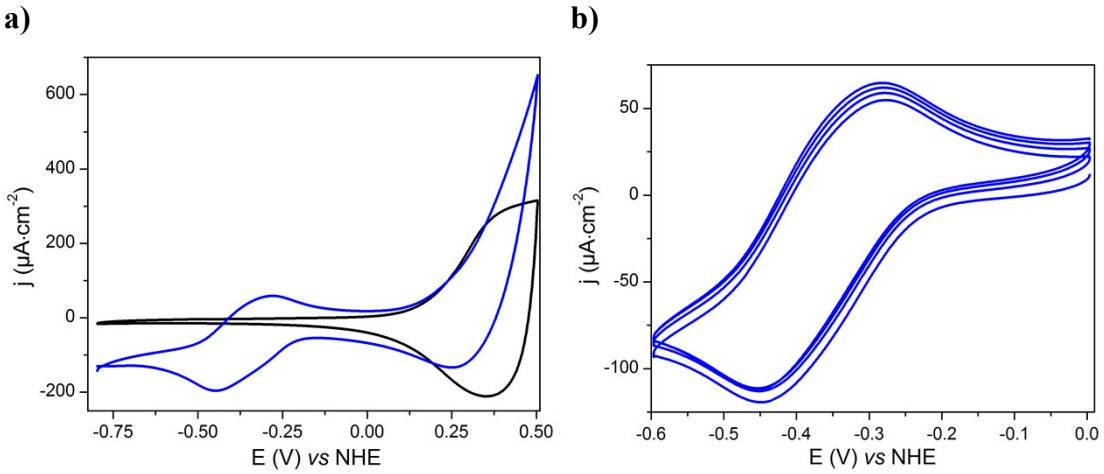

Figure S11. a) CVs recorded at a pristine NiO electrode (black line) and at a **NiO|Co$_{C_{11}P}$** electrode (blue line); b) successive scans in the cathodic region at a **NiO|Co$_{C_{11}P}$** electrode with a scan rate of 100 mV·s^{-1} in a NaCl 0.1 M aqueous electrolyte. The broad wave at ~ 0.3 V *vs* NHE in the CV measured at a pristine NiO electrode is attributed to a surface-confined Ni$^{III/II}$ redox event likely coupled with the exchange of a proton.[1] This feature is also present at the decorated electrode but with a shape slightly modified possibly upon immobilization of the catalyst at the surface.

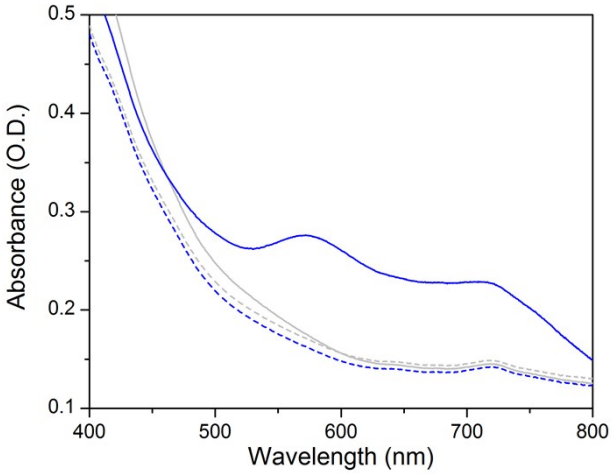

Figure S12. UV-visible spectra of a **NiO|Co$_{C_{11}P}$** electrode (blue lines) and of a pristine NiO electrode (gray lines) poised at –0.24 V *vs* NHE (dotted lines) then at –0.84 V *vs* NHE (plain lines) in a NaCl 0.1 M aqueous electrolyte.

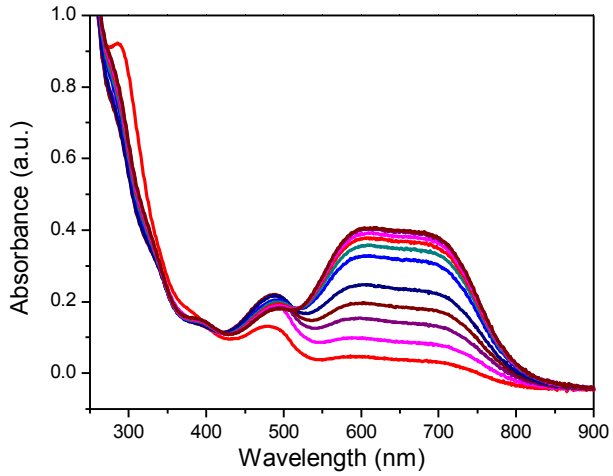

Figure S13. UV-visible spectra of a solution of [Co(DO)(DOH)pnBr$_2$] (1.05 mM in a 0.1M *n*Bu$_4$PF$_6$ solution in MeCN) recorded at a Pt grid electrode poised at – 1 V *vs* Ag/AgCl after 30, 180, 300, 420, 600, 950, 1200, 1300, 1500, 1700, 1800 s (from red to purple) in a H_2O/O_2-free glovebox, with a light path of 1.0 mm.

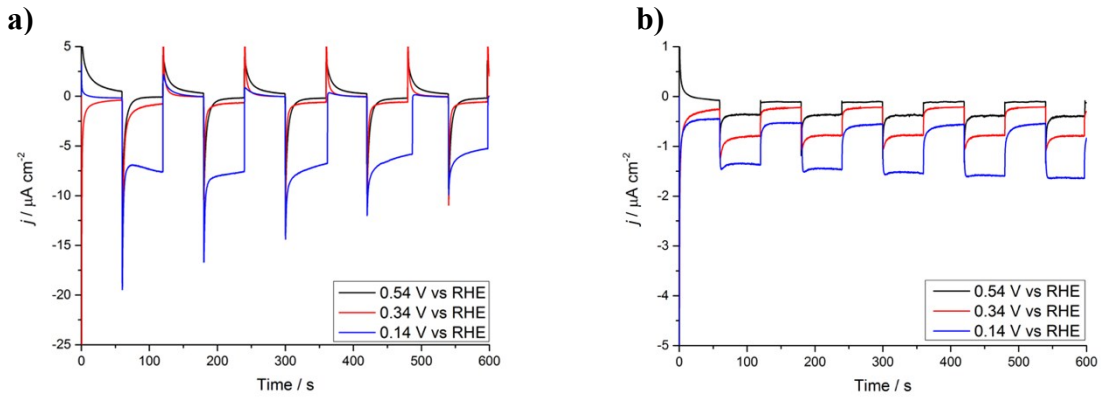

Figure S14. Current densities *vs* time at a) **NiO|RBG-174|Co$_{C_{11}P}$** and b) **NiO|RBG-174|C$_{10}$P** electrodes poised at 0.14 (red line), 0.34 (blue line) and 0.54 (black line) V vs RHE under chopped light irradiation in MES 0.1M / NaCl 0.1 M aqueous electrolyte at pH 5.5.

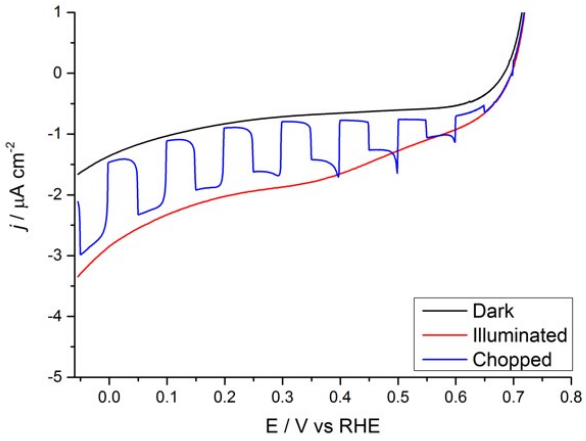

Figure S15. LSVs at a **NiO|RBG-174|C$_{10}$P** electrode with (red line), without (black line) or with chopped (blue line) light irradiation recorded at a scan rate of 10 mV·s^{-1} in MES 0.1M / NaCl 0.1 M aqueous electrolyte at pH 5.5.

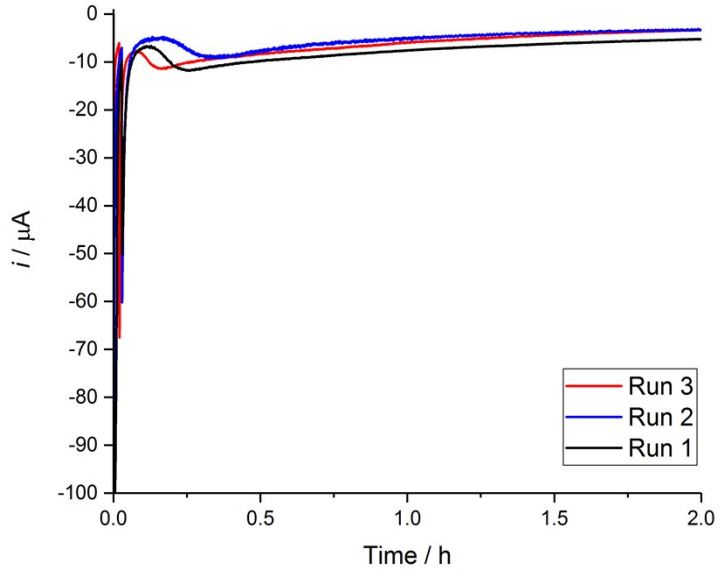

Figure S16. Chronoamperometric measurements performed on three distinct **NiO|RBG-174|Co$_{C_{11}P}$** electrodes under light irradiation recorded at 0.14 V vs RHE in MES 0.1M / NaCl 0.1 M aqueous electrolyte at pH 5.5.

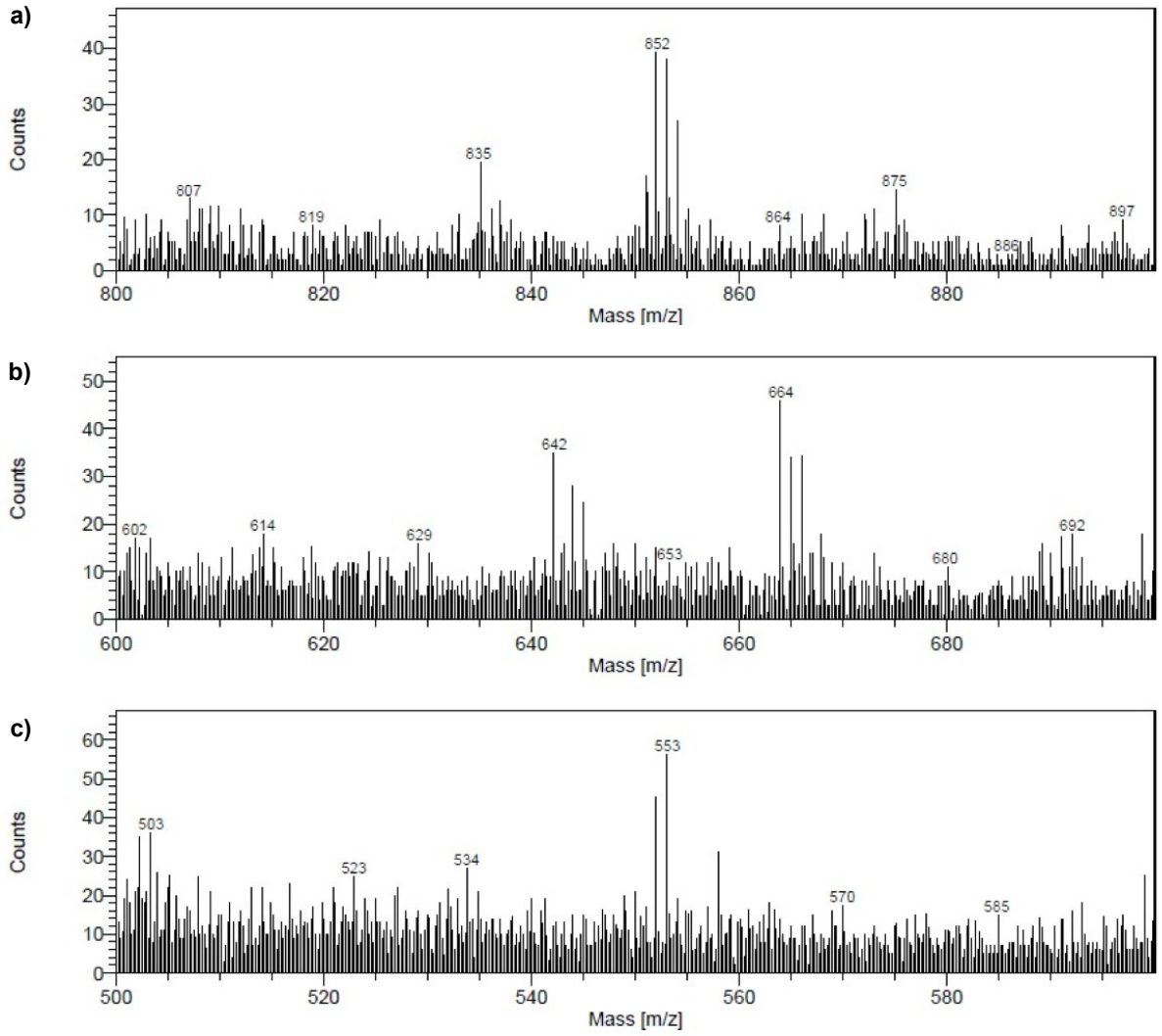

Figure S17. Positive mode ToF-SIMS spectra in the m/z ranges **a)** 800-900, **b)** 600-700 and **c)** 500-600 for the **NiO|RBG-174|$Co_{C_{11}P}$** electrode after two hours of light irradiation poised at E = 0.14 V vs RHE in a MES 0.1 M/NaCl 0.1 M aqueous buffer at pH 5.5.

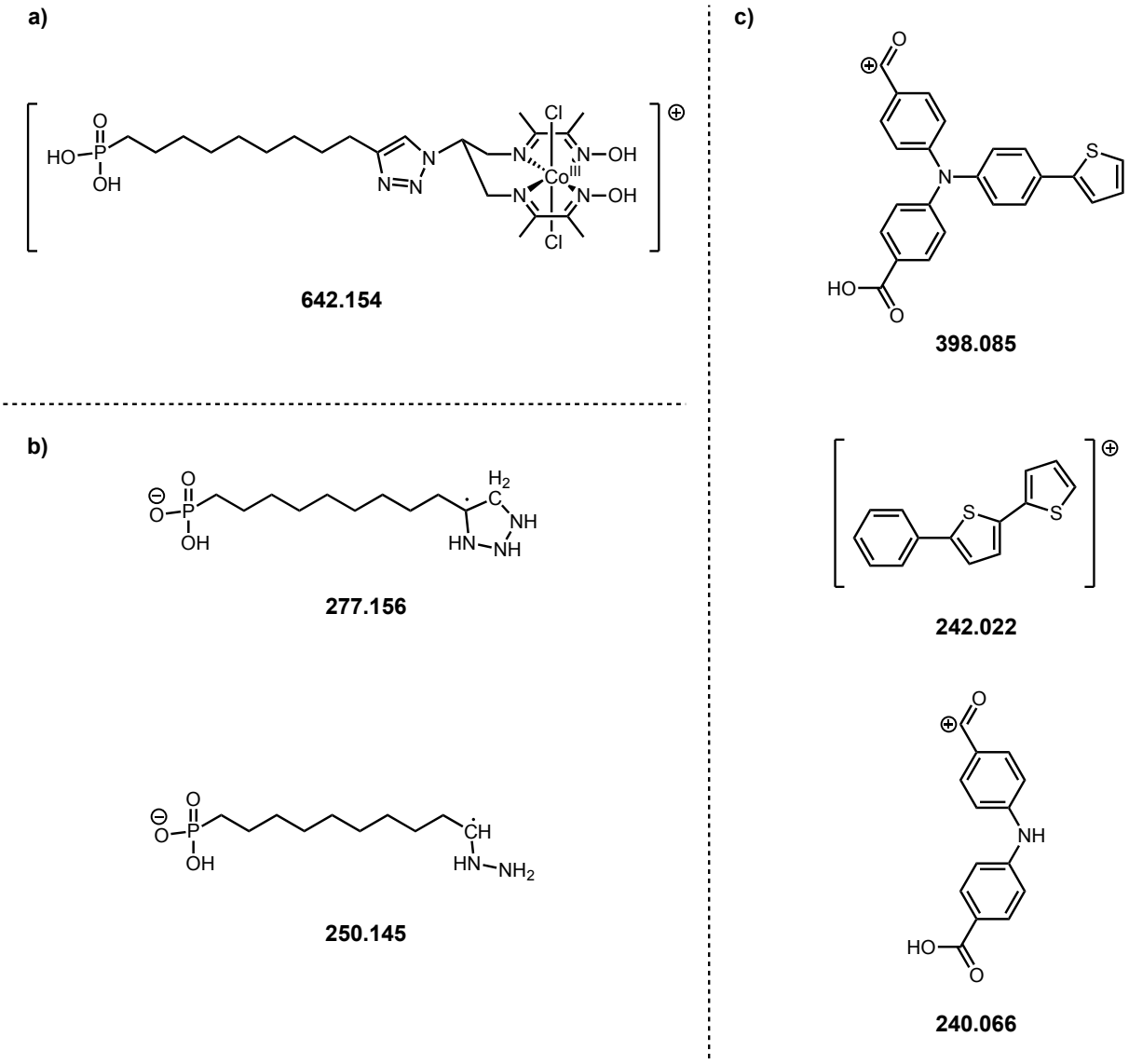

Figure S18. Proposed fragments (with corresponding exact masses) for the attribution of peaks for $\mathbf{Co_{C_{11}P}}$ in a) the positive mode and b) the negative mode and c) for **RBG-174** in the positive mode, in ToF-SIMS spectra at a **NiO|RBG-174|**$\mathbf{Co_{C_{11}P}}$ electrode after two hours of light irradiation poised at E = 0.14 V vs RHE in a MES 0.1 M/NaCl 0.1 M aqueous buffer at pH 5.5.

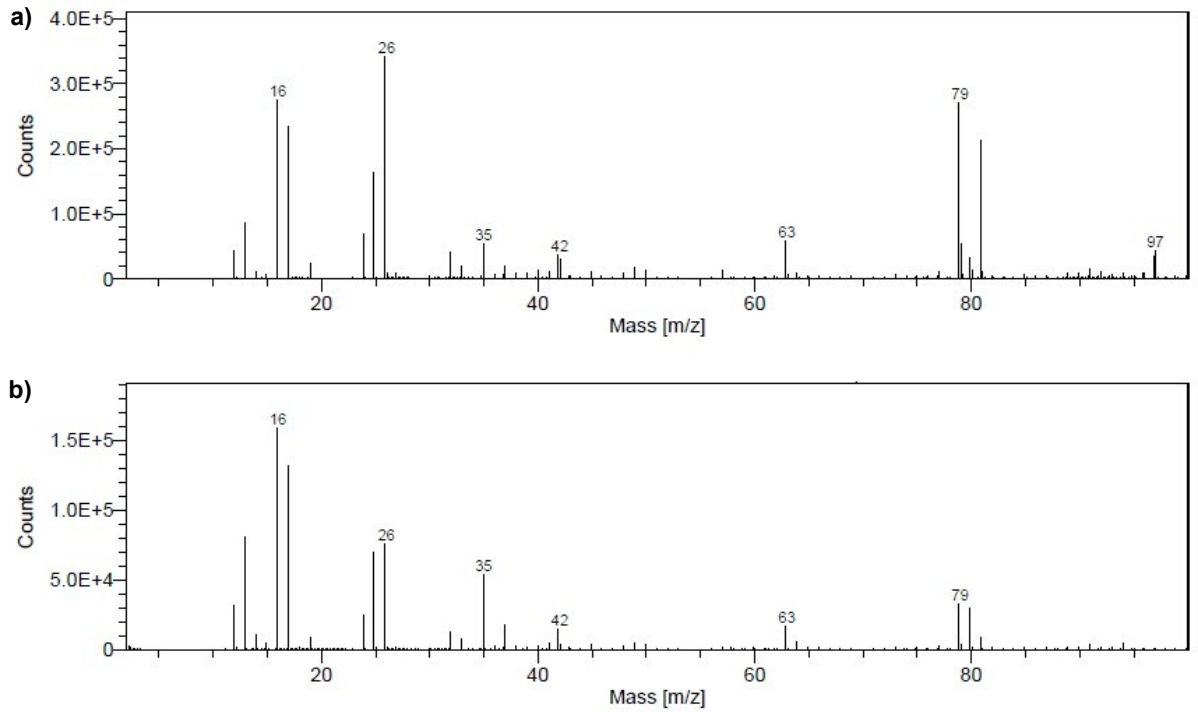

Figure S19. Negative mode ToF-SIMS spectra in the m/z 0-100 range for the **NiO|RBG-174|Co$_{C_{11}P}$** electrode **a)** before and **b)** after two hours of light irradiation poised at E = 0.14 V vs RHE in a MES 0.1 M/NaCl 0.1 M aqueous buffer at pH 5.5.

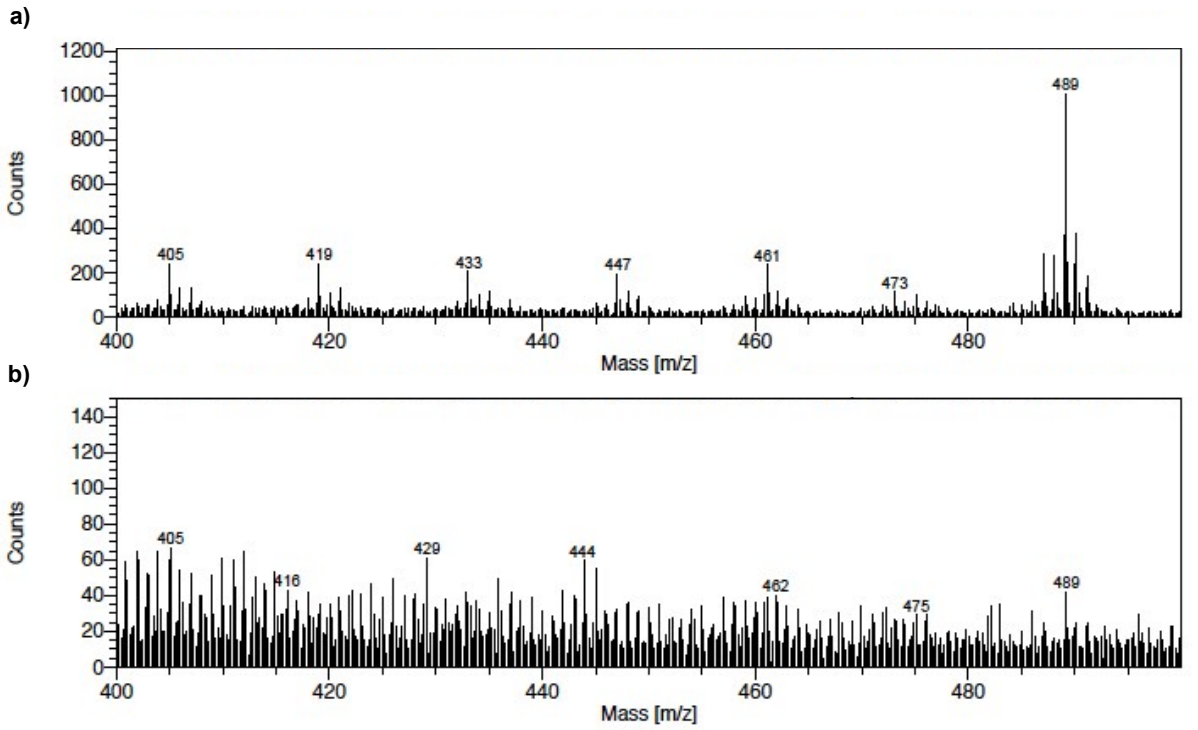

Figure S20. Positive mode ToF-SIMS spectra in the m/z 400-500 range for the **NiO|RBG-174|Co$_{C_{11}P}$** electrode **a)** before and **b)** after two hours of light irradiation poised at E = 0.14 V vs RHE in a MES 0.1 M/NaCl 0.1 M aqueous buffer at pH 5.5.

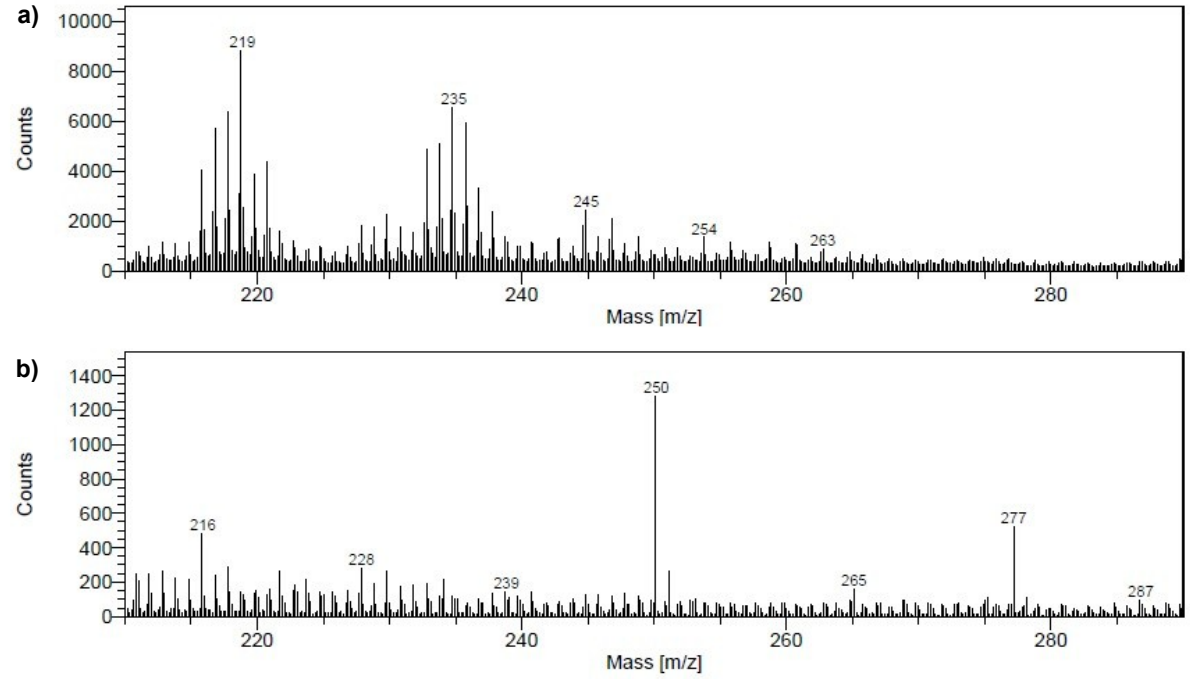

Figure S21. Negative mode ToF-SIMS spectra in the m/z 200-300 range for the **NiO|RBG-174|Co$_{C_{11}P}$** electrode **a)** before and **b)** after two hours of light irradiation poised at E = 0.14 V vs RHE in a MES 0.1 M/NaCl 0.1 M aqueous buffer at pH 5.5.

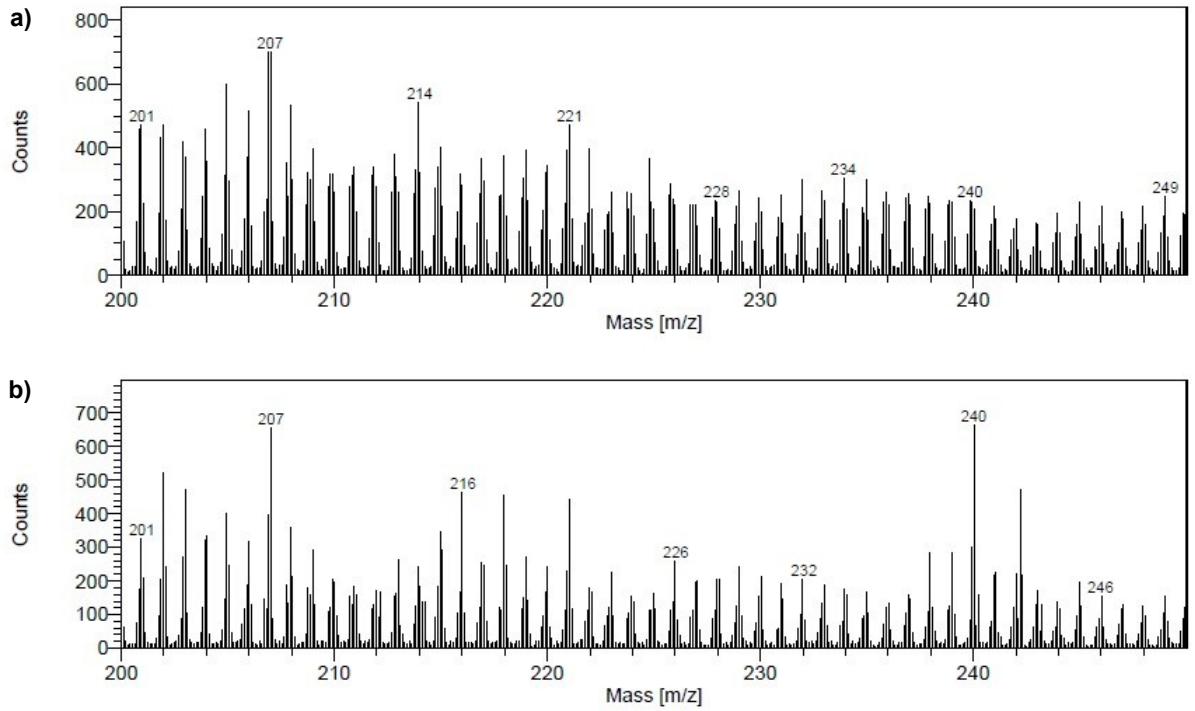

Figure S22. Positive mode ToF-SIMS spectra in the m/z 200-250 range for the **NiO|RBG-174|Co$_{C_{11}P}$** electrode **a)** before and **b)** after two hours of light irradiation poised at E = 0.14 V vs RHE in a MES 0.1 M/NaCl 0.1 M aqueous buffer at pH 5.5.

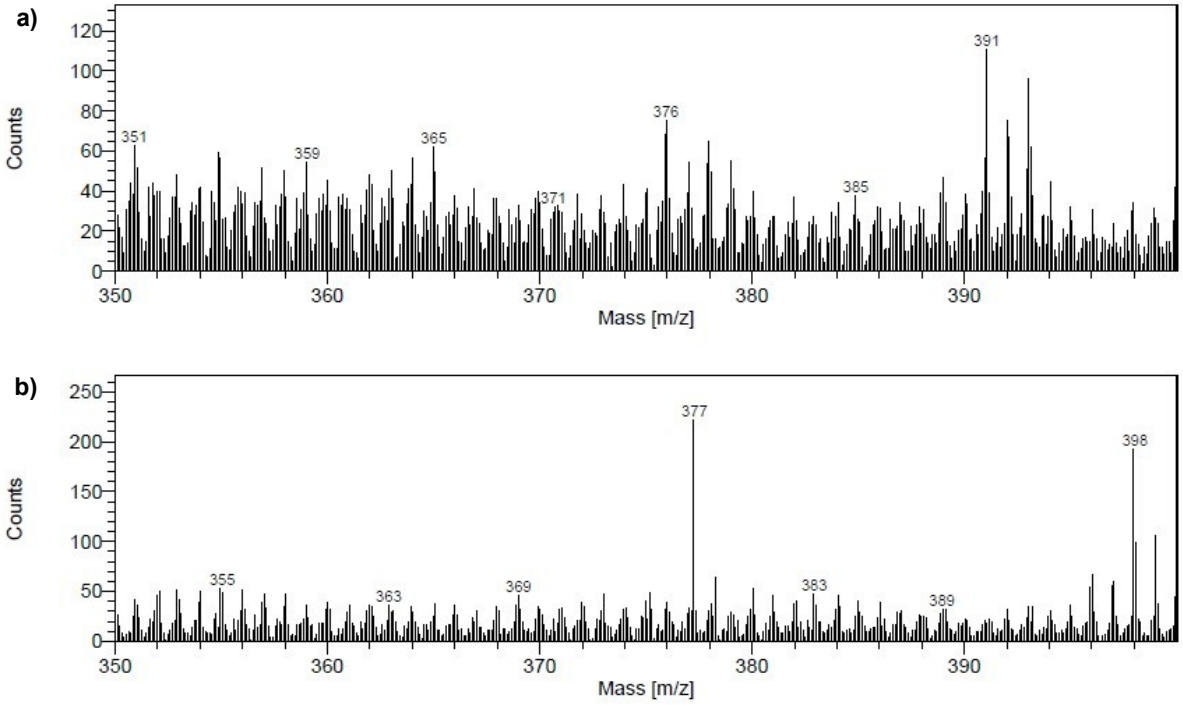

Figure S23. Positive mode ToF-SIMS spectra in the m/z 350-400 range for the **NiO|RBG-174|$Co_{C_{11}P}$** electrode **a)** before and **b)** after two hours of light irradiation poised at E = 0.14 V vs RHE in a MES 0.1 M/NaCl 0.1 M aqueous buffer at pH 5.5.

References

1. (a) Dini, D.; Halpin, Y.; Vos, J. G.; Gibson, E. A., The influence of the preparation method of NiOx photocathodes on the efficiency of p-type dye-sensitized solar cells. *Coord. Chem. Rev.* **2015,** *304-305*, 179-201; (b) Boschloo, G.; Hagfeldt, A., Spectroelectrochemistry of nanostructured NiO. *J. Phys. Chem. B* **2001,** *105* (15), 3039-3044.